LUP

Lund University Publications

Institutional Repository of Lund University

Membrane selectivity by W-tagging of antimicrobial peptides

Artur Schmidtchen[1], Lovisa Ringstad[2], Gopinath Kasetty[1], Hiroyasu Mizuno[3], Mark W. Rutland[3], and Martin Malmsten[2,*]

[1]Division of Dermatology and Venereology, Department of Clinical Sciences, Lund University, SE-221 84 Lund, Sweden.

[2]Department of Pharmacy, Uppsala University, SE-75123, Uppsala, Sweden

[3]Division of Surface and Corrosion Science, Royal Institute of Technology, SE-10044 Stockholm, Sweden.

[*]Corresponding author. Tel: +46184714334; Fax: +46184714377; E-mail: martin.malmsten@farmaci.uu.se

Abstract

A pronounced membrane selectivity is demonstrated for short, hydrophilic, and highly charged antimicrobial peptides, end-tagged with aromatic amino acid stretches. The mechanisms underlying this were investigated by a method combination of fluorescence and CD spectroscopy, ellipsometry, and Langmuir balance measurements, as well as with functional assays on cell toxicity and antimicrobial effects. End-tagging with oligotryptophan promotes peptide-induced lysis of phospholipid liposomes, as well as membrane rupture and killing of bacteria and fungi. This antimicrobial potency is accompanied by limited toxicity for human epithelial cells and low hemolysis. The functional selectivity displayed correlates to a pronounced selectivity of such peptides for anionic lipid membranes, combined with a markedly reduced membrane activity in the presence of cholesterol. As exemplified for GRR10W4N (GRRPRPRPRPWWWW-NH$_2$), potent liposome rupture occurs for anionic lipid systems (dioleoylphosphatidylethanolamine (DOPE)/dioleoylphosphatidylglycerol (DOPG) and *Escherichia coli* lipid extract) while that of zwitterionic dioleoylphosphatidylcholine (DOPC)/cholesterol is largely absent under the conditions investigated. This pronounced membrane selectivity is due to both a lower peptide binding to the zwitterionic membranes ($z \approx -8$-10 mV) than to the anionic ones ($z \approx -35$-40 mV), and a lower degree of membrane incorporation in the zwitterionic membranes, particularly in the presence of cholesterol. Replacing cholesterol with ergosterol, thus mimicking fungal membranes, results in an increased sensitivity for peptide-induced lysis, in analogy to the antifungal properties of such peptides. Finally, the generality of the high membrane selectivity for other peptides of this type is demonstrated.

Introduction

Antimicrobial peptides (AMPs) are currently receiving considerable attention due to increasing antibiotics resistance development, where efforts are directed to identifying potent and selective AMPs, e.g., through quantitative structure-activity relationships or through identification of AMPs of endogenous origin (1-8). Although AMPs influence bacteria in a number of ways, membrane rupture is a key action mechanism for these peptides (2-8). Since bacterial membranes are rich in anionic phospholipids, while human cell membranes are dominated by zwitterionic ones, some AMP selectivity can be obtained for positively charged and hydrophilic AMPs. However, a number of important pathogens, e.g., *Staphylococcus aureus*, display a low electrostatic surface potential, which may be reduced or even reversed (6). Furthermore, due to electrostatic screening, the bactericidal potency of such peptides at physiological ionic strength is typically limited. Through increasing AMP hydrophobicity this inactivation at high ionic strength may be reduced, although highly hydrophobic AMPs have been found to be less selective in their action, thus displaying significant toxicity (4). Given this, we previously identified end-tagging of AMPs with hydrophobic amino acid stretches (10-12) as a way to promote peptide binding and membrane disruption, and to reduce salt sensitivity of AMPs. Such peptides were demonstrated to display limited toxicity combined with high microbicidal potency of broad spectrum, also at physiological ionic strength and in the presence of serum, as well as *ex vivo* and *in vivo*. While it could be demonstrated that the potency of these peptides was due to the hydrophobic end-tagging promoting peptide adsorption at phospholipid membranes, the finer details of the effect of the hydrophobic modifications remained to be elucidated.

Given this, the present study aims to bring this work further by investigating the effects of end-tagging of short, hydrophilic, and highly charged AMPs on peptide incorporation into phospholipid membranes of different composition. In doing so, we employ a method combination of liposome leakage assay, ellipsometry, CD and fluorescence spectroscopy, and Langmuir balance, aimed at elucidating effects of lipid membrane composition on peptide adsorption to, incorporation into, and rupture of the membranes, and how this translates into functional selectivity of these peptides. Using the peptide GRRPRPRPRP (derived from human proline arginine-rich and leucine-rich repeat protein (PRELP) (13)) as an illustrating example, we demonstrate that short, hydrophilic, and highly charged AMPs may display

pronounced selectivity for bacteria and fungi when end-tagged to aromatic amino acid stretches, which can be largely understood as originating from effects of membrane charge, as well as presence and identity of sterol, on peptide-membrane interactions.

Experimental

Peptides. Peptides (Table 1) were synthesized by Biopeptide Co., San Diego, USA, with the exception of LL-37, which was obtained from Innovagen AB, Lund, Sweden. Peptides used were all of >95% purity, as evidenced by mass spectral analysis (MALDI-TOF Voyager). LL-37 (LLGDFFRKSKEKIGKEFKRIVQRIKDFLRNLVPRTES) and omiganan (ILRWPWWPWRRK-NH$_2$) were chosen as control peptides, LL-37 since this is one of the most widely investigated AMPs in literature, and omiganan since this peptide has undergone late stage clinical development and testing, hence a suitable reference peptide from a therapeutic perspective.

Microorganisms. *Escherichia coli* ATCC 25922, *Staphylococcus aureus* ATCC 29213, and *Pseudomonas aeruginosa* ATCC 27853, *Candida albicans* 90028, and *Candida parapsilosis* 90015 clinical isolates were obtained from the Department of Clinical Bacteriology at Lund University Hospital, Sweden.

Radial diffusion assay. Essentially as described previously (14,15), bacteria were grown to mid-logarithmic phase in 10 ml of full-strength (3% w/v) trypticase soy broth (TSB) (Becton-Dickinson, Cockeysville, USA). The microorganisms were then washed once with 10 mM Tris, pH 7.4, with additional 150 mM NaCl. Subsequently, $4x10^6$ colony forming units (cfu) were added to 15 ml of the underlay agarose gel, consisting of 0.03% (w/v) TSB, 1% (w/v) low electroendosmosis type (EEO) agarose (Sigma-Aldrich, St. Louis, USA), and 0.02% (v/v) Tween 20 (Sigma-Aldrich, St. Louis, USA). The underlay was poured into a Ø 144 mm petri dish. After agarose solidification, 4 mm-diameter wells were punched and 6 μl peptide solution of required concentration added to each well. Plates were incubated at 37ºC for 3 hours to allow peptide diffusion. The underlay gel was then covered with 15 ml of molten overlay (6% TSB and 1% Low-EEO agarose in distilled H$_2$O). Antimicrobial activity of a peptide was visualized as a zone of clearing around each well after 18-24 hours of incubation at 37°C.

Viable-count analysis. *S. aureus* ATCC 29213 were grown to mid-logarithmic phase in Todd-Hewitt (TH) medium, while *P. aeruginosa* ATCC 27853 were grown in TH overnight. Bacteria were washed and diluted in 10 mM Tris, pH 7.4, 5 mM glucose, 0.15 M NaCl. 50 µl of 2×10^6 cfu/ml bacteria were incubated at 37°C for 2 hours in the presence of peptide at the indicated concentrations. Serial dilutions of the incubation mixture were plated on TH agar, followed by incubation at 37°C overnight and cfu determination. For further evaluation of bactericidal effects, *P. aeruginosa* ATCC 27853 and *S. aureus* ATCC 29213 were grown to mid-logarithmic phase in Todd-Hewitt (TH) medium. Bacteria were washed and diluted in 10 mM Tris, pH 7.4, 5 mM glucose, 0.15 M NaCl, with 20% human citrate-plasma (50 ml; 2 $\times 10^6$ cfu/ml). After exposure to GRR10W4N, serial dilutions of the incubation mixture were plated on TH agar, followed by incubation at 37°C overnight and cfu determination. In the experiments using 50% whole blood, *S. aureus* ATCC 29213 and *P. aeruginosa* ATCC 27853 bacteria (50 µl; 2×10^8 cfu/ml) were incubated at 37°C for 1 hour in the presence of peptide at 60 and 120 µM. Serial dilutions of the incubation mixture were plated on TH agar, followed by incubation at 37°C overnight and cfu determination.

Minimal inhibitory concentration (MIC) determination. In order to determine the minimal inhibitory concentration (MIC) for a given peptide and bacteria, we used a standardized dilution method according to NCSLA guidelines. In brief, fresh overnight colonies were suspended to a turbidity of 0.5 units and further diluted in Mueller-Hinton broth (MH) (Becton Dickinson). For determination of MIC, peptides were dissolved in water at concentration 10 times higher than the required range by serial dilutions from a stock solution. Ten µl of each concentration was added to each corresponding well of a 96-well microtiter plate (polypropylene, Costar Corp.) and 90 µl of bacteria (1×10^5) in MH medium added. The plate was incubated at 37 °C for 16-18 h. MIC was considered as the lowest concentration where no visual growth of bacteria was detected.

MTT assay. Sterile filtered MTT (3-(4,5-dimethylthiazolyl)-2,5-diphenyl-tetrazolium bromide; Sigma-Aldrich, St. Louis, USA) solution (5 mg/ml in PBS) was stored protected from light at -20°C until usage. HaCaT keratinocytes, 3000 cells/well, were seeded in 96 well plates and grown in keratinocyte-SFM/BPE-rEGF medium to confluence. Keratinocyte-SFM/BPE-rEGF medium alone, or keratinocyte-SFM supplemented with 20% serum, was added, followed by peptide addition to 60 µM. After incubation over night, 20 µl of the MTT

solution was added to each well and the plates incubated for 1 h in CO_2 at 37°C. The MTT-containing medium was then removed by aspiration. The blue formazan product generated was dissolved by the addition of 100 µl of 100% DMSO per well. The plates were then gently swirled for 10 min at room temperature to dissolve the precipitate. The absorbance was monitored at 550 nm, and results given represent mean values from triplicate measurements.

Lactate dehydrogenase (LDH) assay. HaCaT keratinocytes were grown in 96 well plates (3000 cells/well) in serum-free keratinocyte medium (SFM) supplemented with bovine pituitary extract and recombinant EGF (BPE-rEGF) (Invitrogen, Eugene, USA) to confluency. The medium was then removed, and 100 µl of the peptides investigated (at 60 µM, diluted in SFM/BPE-rEGF or in keratinocyte-SFM supplemented with 20% human serum) added in triplicates to different wells of the plate. The LDH-based TOX-7 kit (Sigma-Aldrich, St. Louis, USA) was used for quantification of LDH release from the cells. Results given represent mean values from triplicate measurements, and are given as fractional LDH release compared to the positive control consisting of 1% Triton X-100 (yielding 100% LDH release).

Hemolysis assay. EDTA-blood was centrifuged at 800 g for 10 min, whereafter plasma and buffy coat were removed. The erythrocytes were washed three times and resuspended to 5% in PBS, pH 7.4. For experiments in 50% blood, citrate-blood was diluted (1:1) with PBS. The cells were then incubated with end-over-end rotation for 1 h at 37°C in the presence of peptides (60 or 120 µM). 2% Triton X-100 (Sigma-Aldrich, St. Louis, USA) served as positive control. The samples were then centrifuged at 800 g for 10 min. The absorbance of hemoglobin release was measured at 540 nm and is expressed as % of TritonX-100 induced hemolysis. Results given represent mean values from triplicate measurements. In the experiments with blood infected by bacteria, citrate-blood was diluted (1:1) with PBS. The cells were then incubated with end-over-end rotation for 1 h at 37°C in the presence of peptides (60 and 120 µM) and *S. aureus* (2 x 10^8 cfu/ml) or *P. aeruginosa* (2 x 10^8 cfu/ml) bacteria. For evaluation of hemolysis, samples were then processed as above.

Liposome preparation and leakage assay. The liposomes investigated were either zwitterionic (DOPC/cholesterol 60/40 mol/mol, DOPC/ergosterol 60/40 mol/mol, or DOPC without cholesterol) or anionic (DOPE/DOPG 75/25 mol/mol, or *Eschirichia coli* lipid

extract). DOPG (1,2-dioleoyl-*sn*-Glycero-3-phosphoglycerol, monosodium salt), DOPE (1,2-dioleoyl-*sn*-Glycero-3-phoshoetanolamine), and DOPC (1,2-dioleoyl-*sn*-glycero-3-phoshocholine) were all from Avanti Polar Lipids (Alabaster, USA) and of >99% purity, while cholesterol and ergosterol (both of >99% purity), were from Sigma-Aldrich (St. Louis, USA). In addition, reconstituted lipid membranes were used based on polar extract of *E. coli* with a lipid composition of 67.0% phosphatidylethanolamine, 23.2% phosphatidylglycerol, and 9.8% diphosphatidylglycerol (Avanti Polar Lipids; Alabaster, USA). The lipid mixtures were dissolved in chloroform, after which solvent was removed by evaporation under vacuum overnight. Subsequently, 10 mM Tris buffer, pH 7.4 (with or without 150 mM NaCl), was added together with 0.1 M carboxyfluorescein (CF) (Sigma, St. Louis, USA). After hydration, the lipid mixture was subjected to eight freeze-thaw cycles (not for *E. coli* liposomes) consisting of freezing in liquid nitrogen and heating to 60°C. Unilamellar liposomes of about Ø140 nm were generated by multiple extrusions (30 passages) through polycarbonate filters (pore size 100 nm) mounted in a LipoFast miniextruder (Avestin, Ottawa, Canada) at 22°C. Cryo-TEM shows predominantly unilamellar liposomes, with little multilamellar liposomes and non-closed aggregates. This is compatible with both dynamic light scattering and excellent liposome inclusion stability. Together, these findings indicate efficient membrane closure of the lamellar structure. Untrapped CF was removed by two subsequent gel filtrations (Sephadex G-50, GE Healthcare, Uppsala, Sweden) at 22°C, with Tris buffer (with or without 150 mM NaCl) as eluent. CF release from the liposomes was determined by monitoring the emitted fluorescence at 520 nm from a liposome dispersion (10 µM lipid in 10 mM Tris, pH 7.4). An absolute leakage scale was obtained by disrupting the liposomes at the end of each experiment through addition of 0.8 mM Triton X-100 (Sigma-Aldrich, St. Louis, USA). A SPEX-fluorolog 1650 0.22-m double spectrometer (SPEX Industries, Edison, USA) was used for the liposome leakage assay. Measurements were performed in triplicate at 37 °C.

Fluorescence spectroscopy. Tryptophan fluorescence spectra were determined by a SPEX Fluorolog-2 spectrofluorometer at a peptide concentration of 10 µM. An excitation wavelength of 280 nm was used, while emission spectra were taken between 300 and 450 nm. Measurements were conducted at 37°C while stirring in either 10 mM Tris, pH 7.4, with or without 150 mM NaCl. Where indicated, liposomes (100 µM lipid) were included, incubated with the peptides for one hour before measurements were initiated. Spectra intensities were

normalized to those for 10 mM Tris, pH 7.4, in order to facilitate comparison of spectral maximum positions.

CD spectroscopy. Circular dichroism (CD) spectra were measured by a Jasco J-810 Spectropolarimeter (Jasco, Easton, USA). The measurements were performed in duplicate at 37°C in a 10 mm quartz cuvette under stirring with a peptide concentration of 10 μM. The effect on peptide secondary structure of liposomes at a lipid concentration of 100 μM was monitored in the range 200-260 nm. To account for instrumental differences between measurements, the background value (detected at 250 nm, where no peptide signal is present) was subtracted. Signals from the bulk solution were also corrected for.

Ellipsometry. Peptide adsorption to supported lipid bilayers was studied *in situ* by null ellipsometry, using an Optrel Multiskop (Optrel, Kleinmachnow, Germany) equipped with a 100 mW argon laser. All measurements were carried out at 532 nm and an angle of incidence of 67.66° in a 5 ml cuvette under stirring (300 rpm). Both the principles of null ellipsometry and the procedures used have been described extensively before (16,17). In brief, by monitoring the change in the state of polarization of light reflected at a surface in the absence and presence of an adsorbed layer, the mean refractive index (n) and layer thickness (d) of the adsorbed layer can be obtained. From the thickness and refractive index the adsorbed amount (Γ) was calculated according to (18):

$$\Gamma = \frac{(n - n_0)}{dn/dc} d \qquad (1)$$

where dn/dc is the refractive index increment (0.154 cm^3/g) and n_0 is the refractive index of the bulk solution. Corrections were routinely done for changes in bulk refractive index caused by changes in temperature and excess electrolyte concentration.

The zwitterionic phospholipid bilayers were deposited on silica surfaces (electric surface potential -40 mV and contact angle of <10° (19)) by co-adsorption from a mixed micellar solution containing 60/40 mol/mol DOPC/cholesterol, 60/40 mol/mol DOPC/ergosterol, or DOPC, and n-dodecyl-β-D-maltoside (DDM; ≥98% purity, Sigma-Aldrich, St. Louis, USA), as described in detail previously (17). In brief, the mixed micellar solution was formed by

addition of 19 mM DDM in water to DOPC, DOPC/cholesterol (60/40 mol/mol) or DOPC/ergosterol (60/40) dry lipid films, followed by stirring over night, yielding a solution containing 97.3 mol% DDM. This micellar solution was added to the cuvette at 25°C, and the following adsorption monitored as a function of time. When adsorption had stabilised, rinsing with Milli-Q water at 5 ml/min was initiated to remove mixed micelles from solution and surfactant from the substrate. By repeating this procedure and subsequently lowering the concentration of the micellar solution, stable and densely packed bilayers are formed, with structural characteristics similar to those of bulk lamellar structures of the lipids (17,20).

As sub-bilayer and patchy adsorption resulted from the above mixed micelle approach in the case of the anionic lipid mixture, supported lipid bilayers were generated from liposome adsorption in this case. DOPE/DOPG (75/25 mol/mol) and *E. coli* liposomes were prepared as described above, but the dried lipid films resuspended in Tris buffer only with no CF present. In order to avoid adsorption of peptide directly at the silica substrate through any defects of the supported lipid layer, poly-L-lysine (M_w = 170 kDa, Sigma-Aldrich, St. Louis, USA) was preadsorbed from water prior to lipid addition to an amount of 0.045 ± 0.01 mg/m^2, followed by removal of nonadsorbed poly-L-lysine by rinsing with water at 5 ml/min for 20 minutes. Water in the cuvette was then replaced by buffer containing also 150 mM NaCl, which was followed by addition of liposomes in buffer at a lipid concentration of 20 µM, and subsequently by rinsing with buffer (5 ml/min for 15 minutes) when the liposome adsorption had stabilised. The final layer formed had structural characteristics (thickness 40±10 Å, mean refractive index 1.47±0.026) similar to those of the zwitterionic bilayers, which suggests that a layer fairly close to a complete bilayer is formed. Again, the bilayer build-up was performed at 25°C.

After lipid bilayer formation, temperature was raised and the cuvette content replaced by 10 mM Tris buffer at a rate of 5 ml/min over a period of 30 minutes. After stabilization for 40 minutes, peptide was added to a concentration of 0.01 µM, followed by three subsequent peptide additions to 0.1 µM, 0.5 µM and 1 µM, in all cases monitoring the adsorption for one hour. All measurements were made in at least duplicate.

Langmuir balance

Surface pressure on spread lipid monolayers was monitored by Langmuir balance measurements, using KSV LayerBuilder instrumentation and a Minimicro Teflon® trough

(KSV, Helsinki, Finland) with a maximum area of 8350 mm^2. Two hydrophilic (Delrin) interlinked barriers sliding on top of the trough provide symmetric compression. Trough and barriers were cleaned extensively, first in ethanol, and subsequently in water, and were thereafter dried with filtered nitrogen gas. The trough was then filled with degassed and filtered 10 mM Tris buffer, pH 7.4, and aspirated until no trace of surface contaminants were present, judged from the air-water surface tension. Lipid was dissolved in chloroform and added drop-wise to the interface and the solvent allowed to evaporate. Lipid was added until a surface pressure of about 28 mN/m was reached, after which the monolayer was compressed to a surface pressure of 30 mN/m. After equilibration for 20 minutes for stabilization, 100 μl peptide solution (10 mM Tris, pH 7.4) was added to the subphase to a final peptide concentration of 1.0 μM, and additional surface pressure build-up from peptide incorporated in the phospholipid monolayer monitored. Measurements were performed in duplicate at 25°C, and in an inert nitrogen atmosphere, since it has previously been shown that Langmuir films of phospholipids can be subject to oxidation (21).

Results and discussion

As previously demonstrated for peptides derived from kininogen, end-tagging promotes peptide binding to phospholipid membranes, resulting in increased membrane lysis in both model lipid liposomes and bacteria, only weakly depending on which terminal that was used for end-tagging (10,11). The same applies also to the presently investigated GRR10 peptide, where GRR10W4N potently induces leakage in liposomes at both high and low ionic strength, whereas the non-tagged GRR10 and GRR10N display very limited liposome leakage induction (Supporting Material, Figure S1). (As seen here, amidation of the N-terminus has no effect on the membrane interaction for this peptide, and will not be discussed further.) Investigating effects of lipid membrane composition on liposome rupture for GRR10W4N further demonstrates a striking dependence on the nature of the lipid membrane. Thus, while peptide-induced liposome leakage is quite limited for the zwitterionic DOPC, DOPC/cholesterol, and DOPC/ergosterol membranes, that for the anionic DOPE/DOPG and *E. coli* membranes is much more extensive (Figure 1, as well as Supporting Material, Figure S2). Although qualitatively similar to membrane selectivity displayed by a host of AMPs, quantitatively, the selectivity between anionic and zwitterionic membranes observed for

GRR10W4N is significantly more pronounced, exemplified by results obtained for the benchmark peptides LL-37 and omiganan (Figure 1c-d).

In addition, there is a pronounced influence of the presence of a sterol in the lipid membrane, and of the nature of the sterol. Thus, while peptide-induced liposome leakage reaches a limiting about 35% and 20% for DOPC in the absence of sterol at low and high ionic strength, respectively, the additional presence of cholesterol in the membrane drastically reduces the peptide-induced liposome lysis further, while replacing cholesterol (present in human cell membranes) with ergosterol (present in fungi) results in about the same peptide-induced liposome rupture as that observed for DOPC in the absence of sterol (Figure 1).

Investigating these effects of membrane composition further, peptide adsorption to the lipid membranes was monitored with ellipsometry. As can be seen in Figure 2, there is a close correlation between peptide-induced liposome leakage and peptide adsorption density at the lipid membrane. Thus, the anionic DOPE/DOPG and *E. coli* membranes display high adsorption of GRR10W4N, corresponding to a peptide-to-lipid ratio of about 1:10 at the highest peptide concentration investigated. For the zwitterionic membranes, on the other hand, peptide adsorption is substantially lower, reflecting the lower electrostatic potential of these membranes ($\approx$-8-10 mV compared to -35-40 mV for the anionic membranes (12,20); such a (marginal) electrostatic potential of PC and PE membranes is well established in literature (22,23), and has been ascribed either to the finite separation between the positive and negative charge in the zwitterionic group affecting counterion distribution and resulting in a pKa shift for the phosphate group (24), presence of small amounts of fatty acid impurities from minute phospholipid hydrolysis, or surface anrichment of polarizable anions (25).) Interestingly, however, while DOPC/cholesterol displayed much lower peptide-induced liposome leakage than DOPC and DOPC/ergosterol, a comparable, or even slightly higher adsorption is observed for DOPC/cholesterol than for the other two zitterionic membranes, indicating differences in the degree of membrane incorporation of the adsorbed peptide between these zwitterionic membranes.

In order to investigate these effects further, we performed a series of experiments to address the issue of membrane incorporation. In the first of these, W fluorescence spectra of GRR10W4N were monitored in buffer with and without liposomes present. As can be seen in Figure 3, there are only minor differences between the spectra, small compared to substantial

11

effects observed on peak position and intensity for tryptophans in non-polar environments. Since W fluorescence is highly sensitive to the polarity of the ambient (26), the emission peak at ≈360 nm shows that the W residues of GRR10W4N are exposed to the aqueous solution. Furthermore, CD spectroscopy demonstrates that there is little or no helix-induction in GRR10 or GRR10N in the presence of the phosholipid membrane (helix content for both lipids in Tris buffer and in the presence of DOPE/DOPG or DOPC/cholesterol liposomes 7±2%), excluding ordered transmembrane structures (Figure 4). While the CD spectra for GRR10W4N is complicated due to the CD signal of the W side chain (12), the lack of signal in the 215 nm region suggests that membrane-dependent helix induction is limited also for GRR10W4N. Taken together, fluorescence and CD spectroscopy shows that GRR10W4N binds to phospholipid membranes within, or close to, the polar headgroup region in the membrane. This is in agreement with previous findings that bulky and polarizable W (and F) residues have an affinity to interfaces, and are frequently located in the proximity of the polar headgroup region in phospholipid membranes (27-33). In the case of antimicrobial peptides, related findings have been reported, e.g., by Glukhov et al., demonstrating sequence-dependent penetration of KKKKKKAAXAAWAAXAA (X being W or F) of 2.5-8Å (27), while, Li et al., investigated aurein 1.2 analogs and found the F residues in these peptides to penetrate 2-5Å below the polar headgroup region (28). Also recent NMR findings by Orädd et al. for a W-modified variant of the complement-derived peptide CNY21 support this notion (34).

Monitoring effect of membrane composition on peptide insertion was also monitored more directly by Langmuir balance. As can be seen in Figure 5 and Figure S3 (Supporting Material), GRR10W4N is able to incorporate into both zwitterionic and anionic phospholipid monolayers. As expected, and as previously observed (35-40), peptide incorporation decreases with increasing monolayer pressure (Supporting Material, Figure S3). In analogy with peptide adsorption, peptide incorporation is much more extensive for anionic than for zwitterionic membranes, both therefore contributing to the higher peptide-induced membrane rupture found for the anionic membranes (Figure 5; Supporting Material, Figure 3). A similar more extensive peptide incorporation in anionic phospholipid monolayers was observed by Sanchez-Martin et al. for E1(145-162) hepatitis G virus peptide for dimyrostoylphosphatidylcholine and dimyrostoylphosphatidylglycerol monolayers (36). Similarly, Won and Ianoul found the peptide pEM-2 (KKWRWWLKALAKK) to be more extensively incorporated in anionic monolayers (dioleoylphosphatidylglycerol and *E. coli*

lipid extract) than in a zwitterionic dioleoylphosphatidylcholine monolayer at low surface pressures (7.5 mN/m), as well as continued peptide incorporation (although quantitatively smaller) in the anionic monolayers, but complete exclusion of the peptide from the zwitterionic monolayer at high surface pressure (30 mN/m) (37). Although complicated by peptide self-assembly, a similar increased peptide incorporation with increasing monolayer negative charge was found by Thakur et al. for Aβ (1-40) in palmitoyloleoylphosphatidylcholine/palmitoyloleoylphosphatidylglycerol and dipamitoylphosphatidylcholine/ganglioside GM1 mixed monolayers (38). In the presence of cholesterol, peptide incorporation into DOPC monolayers is further precluded, an effect due to the membrane condensing effects of cholesterol (41-43). For example, Henriksen et al. monitored the effect of sterols on palmityloleoylphosphatidylcholine (POPC) liposomes by micropipette aspiration, and found cholesterol to potently increase the membrane expansion modulus in a concentration-dependent manner, while the effect of ergosterol was much smaller (42). Furthermore, in analogy to the present results (Figure 5) cholesterol has previously been found to reduce peptide incorporation into lipid monolayers. Thus, Azouzi et al. investigated effects of cholesterol content in mixed monolayers for the cyclic peptide cyclosporine A and found the exclusion pressure of this peptide to decrease linearly with the cholesterol content (39). Similarly, Sood et al. found cholesterol to cause a decrease of LL-37 incorporation into stearolyloleoyl monolayers over the entire surface pressure range, as well as the peptide exclusion pressure (40). In line with the overall conclusions from the present investigation, the authors of the latter report summarized the origin of the distinction between target and host cell (although being less pronounced for LL-37 than for the presently investigated peptides (Figure 1)) to originate from a combination of an enhanced peptide binding to anionic phospholipids, and an attenuation of peptide interactions from cholesterol and sphingomyelin. Taken together, the presently reported Langmuir monolayer results are therefore in good agreement with results from investigations previously reported in literature.

The presently observed membrane selectivity is expected to be of relevance for the functional performance of AMPs. Thus, human cell membranes and bacterial membranes have similar functions but differ in composition. For example, in the membrane of red blood cells, phosphatidylcholine (PC) and sphingomyelin (SM) are abundant in the outer layer, while the inner leaflet mainly contains amino lipids (phosphatidylethanolamine (PE) and phosphatidylserine (PS)). These lipids are zwitterionic (except for PS), rendering the outer part of the membrane essentially uncharged. On the contrary, the outer membrane of bacteria

13

is rich in anionic lipids. For example, the cytoplasmic membrane of *E. coli* typically (although varying between strains, between different growth conditions, etc) contains 82% PE, 6% PG, and 12% cardiolipin (44). *S. aureus* membranes, on the other hand, contain PG lipids only, typically of the order 36% PG, 7% cardiolipin, and 57% lysylPG (45). In addition, cholesterol is present in human cell membranes, constituting up to 45% of the total lipids, while it is absent in bacterial membranes, or replaced by ergosterol in fungi. Although these sterols are structurally quite similar, their relative effects on membranes differ substantially. Cholesterol is particularly potent in increasing lipid order in membranes while maintaining fluidity, and provides large mechanical coherence to membranes (39-43). As cholesterol condenses the phospholipid bilayer, peptide adsorption and penetration become sensitive to cholesterol, while ergosterol has more marginal membrane-condensing effects, and confers less stability to phospholipid membranes. Particularly for bulky aromatic groups such as W and F, which require substantial area expansion, insertion into membranes containing cholesterol becomes an energetically costly process. Examples of peptides particularly sensitive to the presence of cholesterol are therefore those containing aromatic oligopeptide residues, such as those discussed here.

Given this difference between cholesterol and ergosterol, identification of peptides which are selective for ergosterol-containing membranes may therefore represent a means to achieve simultaneously antifungal and low-toxic therapeutics. In this context, we previously investigated histidine-rich glycoprotein (HRG) and smaller peptide sequences thereof (46). HRG exerts potent antifungal activity at low pH, mediated via its histidine-rich region, as do small peptides originating from this region. HRG was furthermore found to protect against systemic *Candida* infection *in vivo*, while electron microscopy demonstrated that HRG caused membrane breaks in *Candida* cells and release of cytoplasmic components *in vitro*. In parallel, HRG was found to disrupt liposomes. Notably, ergosterol-containing liposomes, mimicking fungal membranes, were more sensitive than cholesterol-containing ones, mimicking mammalian membranes. Through this selectivity, HRG is able to mediate antifungal effects, at the same time as it displays low toxicity toward human cells.

Although the discussion above has focused on GRR10W4N, we note that high membrane selectivity is a general feature of short, highly charged, and hydrophilic peptides end-tagged with short aromatic amino acid sequences. Thus, GKK10W4, containing lysines rather than arginines as in GRR10W4, provides a similar pronounced selectivity to bacteria-mimicking

DOPE/DOPG membranes over DOPC/cholesterol membranes mimicking mammalian cell membranes (Figure 6a). Similarly, replacing W with F in the end-tags results in a similar preferential membrane lysis (Figure 6b). Taking another peptide sequence altogether of a similar type, i.e., short, highly charged, and hydrophilic (KNK10, KNKGKKNGKH, derived from human kininogen (11)) also results in a similar pronounced selectivity (Figure 6c). Thus, short and hydrophilic peptides containing a high content of positive charges distributed throughout the peptide, combined with aromatic amino acid end-tags seem to provide a general approach for identifying highly selective AMPs.

In order to investigate the possible biological relevance of the selectivity displayed by GRR10W4N and structurally related peptides at the phospholipid membrane level, biological assays were performed to monitor the antimicrobial potency of this peptide, as well as its toxicity to human cell lines. As shown in Figure 7, GRR10W4N indeed displays potent antimicrobial potency against both Gram-positive *S. aureus*, Gram-negative *E. coli* and *P. aeruginosa*, and the fungi *C. albicans* and *C. parapsilosis*, also at the physiological ionic strength under which these measurements were performed. (Analogous results were found for GRR10F5 (Supporting Material, Figure S4), in analogy with the structural generalization demonstrated for liposomes in Figure 6. In addition, the assay independence in regards to the effect of end-tagging was demonstrated by including also data on minimum inhibitory concentration (MIC) (Supporting Material, Table S1), as well as viable count assay data in 10 mM Tris, pH 7.4, 150 mM NaCl, with additional 20% citrate plasma (Supporting Material, Figure S5), the latter demonstrating bactericidal rather than bacteriostatic effects.) Quantitatively, within the limitations of the RDA assay, the antimicrobial effect of GRR10W4N against Gram-negative *E. coli* and Gram-positive *S. aureus* is comparable to that of late phase clinical trials peptide omiganan, and exceeds that of the benchmark peptide LL-37. For Gram-negative *P. aeruginosa*, GRR10W4N was significantly more potent than both benchmark peptides. For the fungi *C. albicans* and *C. parapsilosis*, GRR10W4N displays much stronger inhibitory effects than both omiganan and LL-37. Taken together, the combined data demonstrate the effectiveness of W-tagged AMP against both bacteria and fungi. At the same time, however, toxicity of GRR10W4N to human cells is limited. As shown in Figure 8, GRR10W4N displays very low hemolysis, comparable to that of the negative control, up to 120 µM, as well as low toxicity towards human keratinocytes. Quantitatively, both LDH and MTT assays indicate a toxicity level of GRR10W4N comparable to that of omiganan, particularly clearly seen at 30 µM. For LL-37, both LDH and

15

MTT assays indicate significant toxicity to human keratinocytes as well as human erythrocytes. In order to further illustrate the selectivity of GRR10W4N between bacteria and erythrocytes, citrate-blood was supplemented with either *S. aureus* or *P. aeruginosa*, whereafter peptide was added, and hemolysis and bacteria viable count assays performed on the same sample. As can be seen in Figure 9, LL-37 displays higher hemolysis than the other peptides also in citrate-blood, whereas hemolysis in the presence of the other peptides is comparable to that of the negative control. As expected, GRR10N displays very modest antimicrobial effect against *S. aureus* and *P. aeruginosa* in blood, in agreement with the RDA results for Tris buffer in Figure 7. Also analogous to findings from the simpler RDA assay in buffer, GRR10W4N displays potent antimicrobial effects against *S. aureus*, which exceed those of omiganan and LL-37, while for *P. aeruginosa*, antimicrobial effects for GRR10W4N and LL-37 are comparable, and significantly stronger than that of omiganan. Taken together, the data in Figure 7-9 demonstrates a striking selectivity for GRR10W4N, with potent broad spectrum effects combined with low cell toxicity. They also show that the selectivity displayed by GRR10W4N on the phospholipid membrane level translates to a pronounced membrane selectivity on the microbial/cellular level.

As a final point, we note the structural similarity between the presently investigated peptides and that of other P- and R-rich peptides, such as Bac7 peptides (47), prophenin (48-50), and tritrypticin (51,52). As reported, e.g., by Scocchi et al., some of these peptides act also in a non-lytic manner, having an active transport system for membrane passage, and being selectively active on Gram-negative bacteria (47). Although such mechanisms cannot be excluded at present for GRR10W4N and related peptides, we note that i) similar bactericidal effects are observed also for Gram-positive *S. aureus* and the fungus *C. albicans*, and ii) there is a good correlation between bactericidal effect and liposome rupture, both arguing against substantial non-lytic internalization processes.

Conclusions

Increasing antimicrobial peptide hydrophobicity through end-tagging with oligotryptophan promotes peptide-induced lysis of phospholipid liposomes, as well as bacterial and fungal killing. For short, hydrophilic, and highly charged peptides, bactericidal potency after end-tagging is accompanied by limited toxicity for human cells, as well as low hemolysis. A

strikingly selective targeting of bacteria membrane was demonstrated in experiments where bacteria-supplemented blood was exposed to peptides. The functional selectivity thus displayed is, at least in part, due to a pronounced selectivity of such peptides for anionic lipid membranes, combined with sensitivity to the presence of cholesterol. As demonstrated for GRR10W4N (GRRPRPRPRPWWWW-NH$_2$), potent liposome rupture occurs for anionic lipid systems (DOPE/DOPG and *E. coli* lipid extract) while that of zwitterionic DOPC/cholesterol ones is largely absent under the conditions investigated. This striking membrane selectivity is due to a combination of a lower peptide binding density to the zwitterionic membranes (z≈-8-10 mV) than to the anionic ones (z≈-35-40 mV), and a lower degree of peptide insertion into the membrane for the zwitterionic membrane, particularly in the presence of cholesterol, which opposes the substantial area expansion required to incorporate the peptide at these concentrations, particularly since the W-residues also after membrane incorporation remain within (as opposed to on top of), the polar headgroup region. Removing cholesterol, or more interestingly replacing cholesterol with ergosterol, thus mimicking fungal membranes, results in an increased sensitivity for peptide-induced lysis, and demonstrates a possibility for antifungal peptides displaying limited toxicity, also supported directly by antifungal and toxicity data. Given the importance of lipid rafts in many contexts of membrane biochemistry and biophysics, it would be interesting to investigate effects of cholesterol in the presence of sphingomyelin and raft formation. However, with numerous intricacies relating to, e.g., sterol and sphingomyelin structure, but also to acyl length, saturation, branching, and assymetry, as well as to the polar headgroup, of phospholipid components in the membrane, not to mention composition of the 3+-component system, doing these complex issues justice requires a separate investigation. Finally, W-tagging of short, hydrophilic, and highly charged AMPs seems to be a general approach for designing simultaneously potent and low-toxic AMPs.

Acknowledgement

Supporting material

Results on effects of W-tagging on liposome lekage induction, on leakage induction in *E. coli* liposomes by GRR10N and GRR10W4N, data on effects of surface pressure on incorporation of GRR10W4N in DOPE/DOPG and DOPC monolayers, VCA data for GRR10W4N in buffer containing 20% citrate plasma, RDA data for GRR10F5, and MIC values for GRR10W4N, GRR10F5, and control peptides are available as supporting material.

References

1. French, G.L. (2005) Clinical impact and relevance of antibiotic resistance. *Adv. Drug Deliv. Rev.* **57**, 1514-1527.

2. Zasloff, M. (2002) Antimicrobial peptides of multicellular organisms. *Nature* **415**, 389-395.

3. Marr, A.K., Gooderham, W.J., and Hancock, R.E. (2006) Antibacterial peptides for therapeutic use: obstacles and realistic outlook. *Curr. Opin. Pharmacol.* **6**, 468-472.

4. Tossi, A., Sandri, L., and Giangaspero, A. (2000) Amphipathic, alpha-helical antimicrobial peptides. *Biopolymers* **55**, 4-30.

5. Brogden, K.A. (2005) Antimicrobial peptides: pore formers or metabolic inhibitors in bacteria? *Nat. Rev. Microbiol.* **3**, 238-250.

6. Nizet, V. (2006) Antimicrobial peptide resistance mechanisms of human bacterial pathogens. *Curr. Issues Mol. Biol.* **8**, 11-26.

7. Huang, H.W. (2006) Molecular mechanism of antimicrobial peptides: the origin of cooperativity. *Biochim. Biophys. Acta* **1758**, 1292-1302.

8. Hancock, R.E. and Sahl, H.G. (2006) Antimicrobial and host-defense peptides as new anti-infective therapeutic strategies. *Nat. Biotechnol.* **24**, 1551-1557.

9. Strömstedt, A.A., Ringstad, L., Schmidtchen, A., and Malmsten, M. (2010) Interaction between amphiphilic peptides and phospholipid membranes. *Curr. Opin. Colloid Interface Sci*. **2011**, 15, 467-478.

10. Schmidtchen, A., Pasipuleti, M., Mörgelin, M., Davoudi, M., Alenfall, J., Chalupka, A. and Malmsten, M. (2009) Boosting antimicrobial peptides by hydrophobic amino acid end-tags. *J. Biol. Chem.* **284**, 17584-17594.

11. Pasupuleti, M., Schmidtchen, A., Chalupka, A., Ringstad, L., and Malmsten, M. (2009) End-tagging of ultra-short antimicrobial peptides by W/F stretches to facilitate bacterial killing. *PLoS One* **4**, 1-9.

12. Strömstedt, A.A., Pasupuleti, M., Schmidtchen, A., and Malmsten, M. (2009) Oligotryptophan-tagged antimicrobial peptides and the role of the cationic sequence. *Biochim. Biophys. Acta* **1788**, 1916-1923.

13. Malmsten, M., Davoudi, M., and Schmidtchen, A. (2006) Bacterial killing by heparin-binding peptides from PRELP and thrombospondin. *Matrix Biol.* **25**, 294-300.

14. Lehrer, R. I., Rosenman, M., Harwig, S. S., Jackson, R., and Eisenhauer, P. (1991) Ultrasensitive assays for endogenous antimicrobial polypeptides, *J. Immunol. Methods* **137**, 167-173.

15. Andersson, E., Rydengard, V., Sonesson, A., Mörgelin, M., Bjorck, L., and Schmidtchen, A. (2004) Antimicrobial activities of heparin-binding peptides, *Eur. J. Biochem.* **271**, 1219-1226.

16. Malmsten, M. (1994) Ellipsometry studies of protein layers adsorbed at hydrophobic surfaces. *J. Colloid Interface Sci.* **166**, 333-342.

17. Tiberg, F., Harwigsson, I., and Malmsten, M. (2000) Formation of model lipid bilayers at the silica-water interface by co-adsorption with non-ionic dodecyl maltoside surfactant. *Eur. Biophys. J.* **29**, 196-203.

18. De Feijter, J.A., Benjamins, J., and Veer, F.A. (1978) Ellipsometry as a tool to study the adsorption behavior of synthetic and biopolymers at the air-water interface. *Biopolymers* **17**, 1759-1772 .

19. Malmsten, M., Burns, N., and Veide, A. (1998) Electrostatic and hydrophobic effects of oligopeptide insertions on protein adsorption. *J. Colloid Interface Sci.* **204**, 104-111.

20. Ringstad, L., Schmidtchen, A., and Malmsten, M. (2006) Effect of peptide length on the interaction between consensus peptides and DOPC/DOPA bilayers. (2006) *Langmuir* **22**, 5042-5050.

21. Liljeblad, J.F.D., Bulone, V., Tyrode, E., Rutland, M.W., and Johnson, C.M. (2010) Phospholipid monolayers probed by vibrational sum frequency spectroscopy: instability of unsaturated phospholipids. *Biophys. J.* **98**, L50-L52.

22. Matos, C., de Castro, B., Gameiro, P., Lima, J.L.F.C., and Reis, S. (2004) Zeta-potential measurements as a tool to quantify the effect of charged drugs on the surface potential of egg phosphatidylcholine liposomes. *Langmuir* **20**, 369-377.

23. Roy, M.T., Gallardo, M., and Estellrich, J. (1998) Influence of size on electrokinetic behavior of phosphatidylerine and phosphatidylethanolamine lipid vesicles. *J. Colloid Interface Sci.* **206**, 512-517.

24. Moncelli, M.R., Becucci, L., and Guidelli, R. (1994) The intrinsic pK_a values for phosphatidylcholine, phosphatidylethanolamine, and phosphatidylserine in monolayers deposited on mercury electrodes. *Biophys. J.* **66**, 1969-1980.

25. Boström, M., Williams, D.R.M., and Ninham, B.W. (2001) Surface tension of electrolytes: specific ion effects explained by dispersion forces. *Langmuir* **17**, 4475-4478.

26. Lotte, K., Plessow, R., and Brockhinke, A. (2004) Static and time-resolved fluorescence investigations of tryptophan analogues--a solvent study. *Photochem. Photobiol. Sci.* **3**, 348-359.

27. Glukhov, E., Stark, M., Burrows, L.L., and Deber, C.M. (2005) Basis for selectivity of cationic antimicrobial peptides for bacterial versus mammalian membranes. *J. Biol. Chem.* **280**, 33960-33967.

28. Li, X., Li, Y., Peterkofsky, A., and Wang, G. (2006) NMR studies of aurein 1.2 analogs. *Biochim. Biophys. Acta* **1758**, 1203-1214.

29. Hanley, E.F., Lau, F., and Vogel, H.J. (2007) Solution structures and mode membrane interactions of lactoferrampin, an antimicrobial peptide derived from bovine lactoferrin. *Biochim. Biophys. Acta* **1768**, 2355-2364.

30. McInturff, J.E., Wang, S.-J., Machleidt, T., Lin, T.R., Oren, A., Hertz, C.J., Krutzik, S.R., Hart, S., Zeh, K., Anderson, D.H., Gallo, R.L., Modlin, R.L., and Kim, J. (2005) Granulysin-derived peptides demonstrate antimicrobial and anti-inflammatory effects against *Propionibacterium acnes*. *J. Invest. Dermatol.* **125**, 256-263.

31. Deslouches, B., Phadke, S.M., Lazarevic, V., Cascio, M., Islam, K., Montelaro, R.C., and Mietzner, T.A. (2005) *De novo* generation of cationic antimicrobial peptides: influence of length and tryptophan substitution on antimicrobial activity. *Antimicrob. Agents Chemother.* **49**, 316-322.

32. de Planque, M.R.R., Kruijtzer, J.A.W., Liskamp, R.M., Marsh, D., Greathouse, D.V., Koeppe, R.E., de Kruijff, B., and Killian, J.A. (1999) Different membrane anchoring positions of tryptophan and lysine in synthetic transmembrane α-helical peptides. *J. Biol. Chem.* **274**, 20839-20846.

33. Andrushchenko, V.V., Vogel, H.J., and Prenner, E.J. (2007) Interactions of tryptophan-rich cathelicidin antimicrobial peptides with model membranes studied by differential scanning calorimetry. *Biochim. Biophys. Acta* **1768**, 2447-2458.

34. Orädd, G., Schmidtchen, A., and Malmsten, M. (2010) Effects of peptide hydrophobicity on its incorporation in phospholipid membranes – an NMR and ellipsometry study. *Biochim. Biophys. Acta* **2011**, 1808, 244.

35. Arseneault, M., Bédard, S., Boulet-Audet, M., Pézolet, M. (2010) Study of the interaction of lactoferricin B with phospholipid monolayers and bilayers. *Langmuir*

26, 3468-3478.

36.   Sanchez-Martin, M.J., Haro, I., Alsina, M.A., Busquets, M.A., and Pujol, M. (2010) A Langmuir monolayer study of the interaction of E1(145-162) hepatitis G virus peptide with phospholipid membranes. *J. Phys. Chem. B* **114**, 448-456.

37.   Won, A. and Ianoul, A. (2009) Interactions of antimicrobial peptide from C-terminus of myotoxin II with phospholipid mono- and bilayers. *Biochim. Biophys. Acta* **1788**, 2277-2283.

38.   Thakur, G., Micic, M., and Leblanc, R.M. (2009) Surface chemistry of Altzheimer's disease: A Langmuir monolayer approach. *Colloids Surf. B* **74**, 436-456.

39.   Azouzi, S., El Kirat, K., and Morandat, S. (2009) The potent antimalarial drug cyclosporine A preferentially destabilizes sphingomyelin-rich membranes. *Langmuir* **26**, 1960-1965.

40.   Sood, R., Domanov, Y., Pietiänen, M., Kontinen, V.P., and Kinnunen, P.K.J. (2008) Binding of LL-37 to model biomembranes: Insight into target vs host cell recognition. *Biochim. Biophys. Acta* **1778**, 983-996.

41.   Mouritsen, O.G. and Zuckermann, M.J. (2004) What's so special about cholesterol? *Lipids* **39**, 1101-1113.

42.   Henriksen, J., Rowat, A.C., Brief, E., Hsueh, Y.W., Thewalt, J.L., Zuckermann, M.J., and Ipsen, J.H. (2006) Universal behavior of membranes with sterols. *Biophys. J.* **90**, 1639-1649.

43.   Ohvo-Rekilä, H., Ramstedt, B., Leppimäki, P., and Slotte, P. (2002) Cholesterol interactions with phospholipis in membranes. *Progr. Lipid Res.* **41**, 66-97.

44.   Lugtenberg, E.J.J. and Peters, R. (1976) Distribution of lipids in cytoplasmic and outer membranes of Escerichia coli K12, *Biochim. Biophys. Acta* **441**, 38-47.

45.   Haest, C.W., de Gier, J., den Kamp, J.A., Bartels, P., and van Deenen, L.L. (1972) Changes in permeability of Staphylococcus aureus and derived liposomes with varying lipid composition. *Biochim. Biophys. Acta* **255**, 720-733.

46.   Rydengård, V., Shannon, O., Lundqvist, K., Kacprzyk, L., Chalupka, A., Olsson, A.-K., Mörgelin, M., Jahnen-Dechent, W., Malmsten, M., and Schmidtchen, A. (2008) Histidine-rich glycoprotein protects from systemic Candida infection. *PLoS Pathogens* **4**, e1000116, 1-11.

47.   Benicasa, M., Pelillo, C., Zoret, S., Garrovo, C., Biffi, S., Gennaro, R., and Scocchi, M. (2010) The proline-rich peptide Bac7(1-35) reduces mortality from Salmonella typhimurium in a mouse infection model. *BMC Microbiology* **10:178**, 1-8.

48. Wang, Y., Griffiths, W.J., Curstedt, T., and Johansson, J. (1999) Porcine pulmonary preparations contain the antibacterial peptide prophenine and a C-terminal 18-residue fragment thereof. *FEBS Letts*. **460**, 257-262.

49. Wang, Y., Johansson, J., and Griffiths, W.J. (2000) Characterisation of variant forms of prophenin: mechanistic aspects of the fragmentation of proline-rich peptides. *Rapid Comm. Mass Spectrom.* **14**, 2182-2202.

50. Harwig, S.S.L., Kokryakov, V.N., Swiderek, K.M., Aleshina, G.M., Zhao, C., and Lehrer, R.I. (1995) Prophenin-1, an exceptionally proline-rich antimicrobial peptide from porcine leukocytes. *FEBS Letts*. **362**, 65-69.

51. Nagpal, S., Gupta, V., Kaur, K.J., and Salunke, D.M. (1999) Structure-function analysis of tritrypticin, an antibacterial peptide of innate immune origin. *J. Biol. Chem.* **274**, 23296-23304.

52. Kaur, K.J., Sarkar, P., Nagpal, S., Khan, T., and Salunke, D.M. (2008) Structure-function analyses involving palindromic analogs of tritrypticin suggest autonomy of anti-endotoxin and antibacterial activities. *Protein Sci.* **17**, 545-554.

53. Eisenberg, D., Schwarz, E., Komaromy, M., and Wall, R. (1984) Analysis of membrane and surface protein sequences with the hydrophobic moment plot. *J. Mol. Biol*. **179**, 125-142.

Table 1. Primary structure and key properties of the peptides investigated.

	Sequence	IP	Z_{net}[2] (pH 7.4)	H[3]
GRR10	GRRPRPRPRP	12.60	+5	-0.89
GRR10N	GRRPRPRPRP-NH$_2$	12.60	+5	-0.89
GRR10W4N	GRRPRPRPRPWWWW-NH$_2$	12.60	+5	-0.53
GKK10W4N	GKKPKPKPKPWWWW	10.60	+5	-0.29
GRR10F5	GRRPRPRPRPFFFFF	12.60	+5	-0.39
KNK10W3	KNKGKKNGKHWWW	10.60	+5	-0.44
LL-37	LLGDFFRKSKEKIGKEFKRIVQRIKDFLRNLVPRTES	11.09	+6	-0.34
Omiganan	ILRWPWWPWRRK-NH$_2$	12.64	+4	-0.31
WWW	WWW	6.0	-1	0.81

[1] IP:isoelectric point; [2]Z_{net}: net charge; ^{3}H mean hydrophobicity on the Eisenberg scale (53).

Figure Captions

Figure 1 Peptide-induced liposome leakage for GRR10W4N at 10 mM Tris, pH 7.4, in the absence (a) and presence (b) of 150 mM NaCl. Shown also are corresponding data for benchmark peptides LL-37 (c) and omiganan (d).

Figure 2 Adsorption of GRR10W4N to lipid bilayers in 10 mM Tris, pH 7.4. The adsorption of the WWW tripeptide alone was less than 40 nmol/m^2 throughout.

Figure 3 Tryptophan fluorescence spectra, at a peptide concentration of 10 μM, for GRR10W4N in 10 mM Tris, pH 7.4, with or without additional 150 mM NaCl, in the presence and absence of (a) DOPE/DOPG (75/25 mol/mol) or (b) DOPC/cholesterol (60/40 mol/mol) liposomes (100 μM lipid).

Figure 4 CD spectra for GRR10 (a), GRR10N (b), GRR10W4N (c), and WWW (d) in 10 mM Tris, pH 7.4, with or without DOPE/DOPG (75/25 mol/mol) or DOPC/cholesterol (60/40 mol/mol) liposomes (100 μM lipid).

Figure 5 Penetration of GRR10W4N to DOPC, DOPC/cholesterol (60/40 mol/mol), and DOPE/DOPG (75/25 mol/mol) monolayers from Tris buffer, pH 7.4. Surface pressure prior to peptide addition was 30 mN/m.

Figure 6 Generalization of the high selectivity displayed by short, hydrophilic, and highly charged AMPs modified with aromatic oligopeptide end-tags. Shown are liposome results obtained for another charged group (GKKPKPKPKPWWWW) (a), for another aromatic amino acid end-tag (GRRPRPRPRPFFFFF) (b), and for a different peptide sequence (KNKGKKNGKHWWW), derived from kininogen instead of PRELP (c). In (b) and (c), results are shown for 10 mM Tris buffer, pH 7.4, with additional 150 mM NaCl.

Figure 7 Antimicrobial effect, as determined by radial diffusion assay (RDA) in 10 mM Tris, pH 7.4, with additional 150 mM NaCl, of GRR10W4N (10 and 50 μM) against Gram-positive *S. aureus*, and Gram-negative *P. aeruginosa* and *E. coli*, and fungi *C. albicans* and *C. parapsilosis* clinical isolates. For comparison, corresponding data for the control peptides GRR10, GRR10N, LL-37, and omiganan are included as well. In RDA, peptides are placed in

wells in agar gels containing confluent microbes. On radial diffusion, the peptide will kill bacteria and result in a clearance zone containing disintegrated microbes. Thus, the higher the diameter (d), the higher the growth inhibition, i.e., the more potent the peptide.

Figure 8 Cytotoxicity of GRR10W4N, monitored by hemolysis, LDH release, and MTT assay. For comparison, data for the control peptides GRR10, GRR10N, LL-37 and omiganan are included as well.

Figure 9 Combined hemolysis (a) and VCA assay (b) for *S. aureus* and *P. aeruginosa* (both 2 x 10^8 cfu/ml) added to 50% citrate blood, at the indicated peptide concentrations.

Figure 1.

(a)

(b)

(c)

Leakage (%)

- □ DOPE/DOPG Tris
- ○ DOPE/DOPG Tris+NaCl
- ■ DOPC/Chol Tris
- ● DOPC/Chol Tris+NaCl

Concentration (μM)

(d)

Leakage (%)

- □ DOPE/DOPG Tris
- ○ DOPE/DOPG Tris+NaCl
- ■ DOPC/Chol Tris
- ● DOPC/Chol Tris+NaCl

Concentration (μM)

Figure 2.

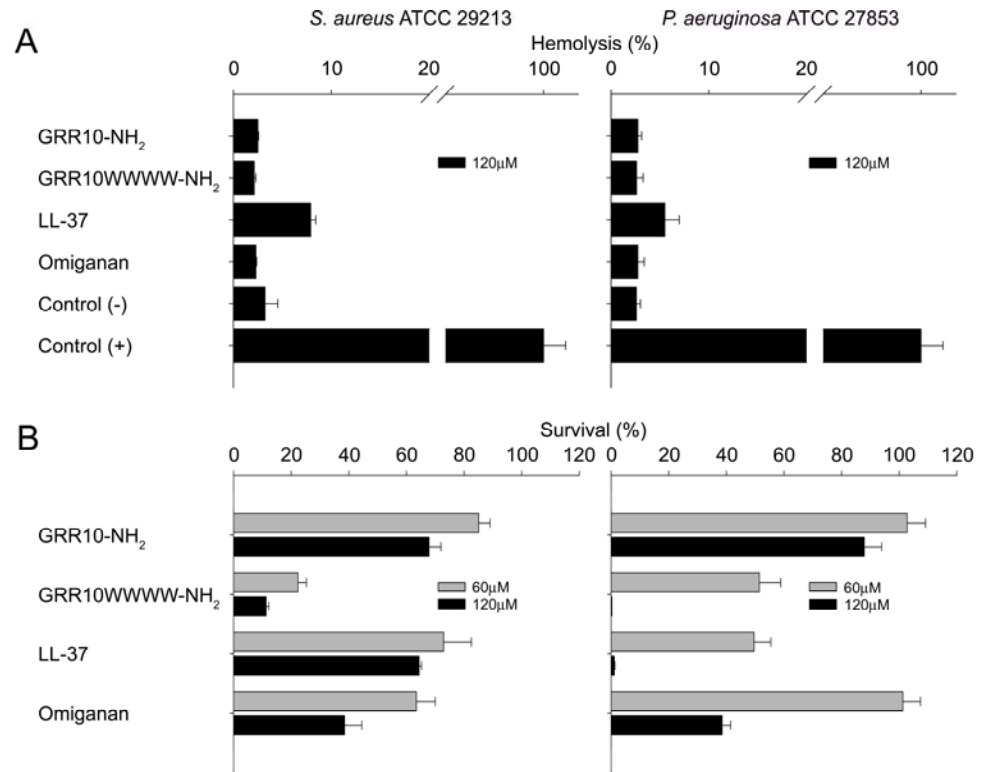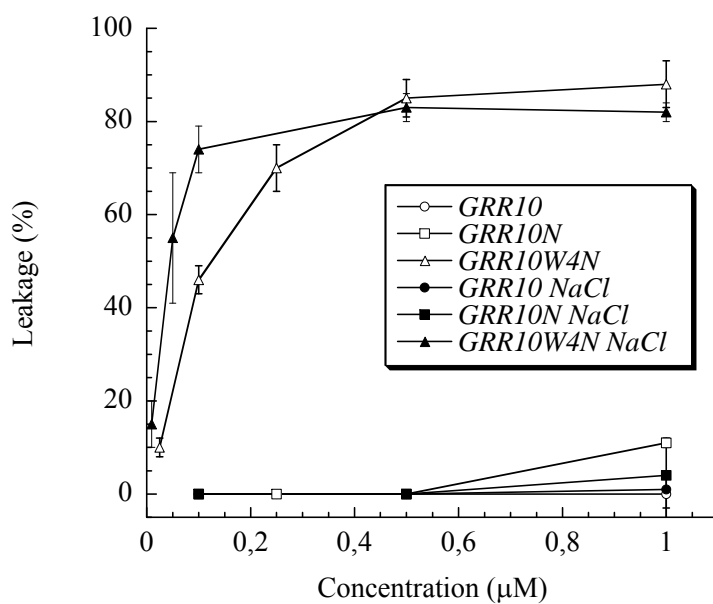Figure 3.

(a)

(b)

Figure 4.

(a)

(b)

(c)

(d)

Figure 5.

Figure 6.

(c)
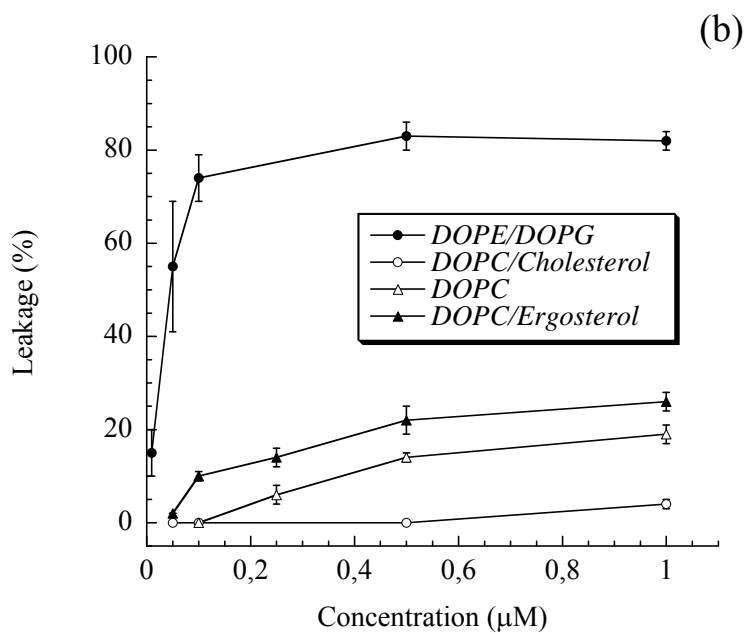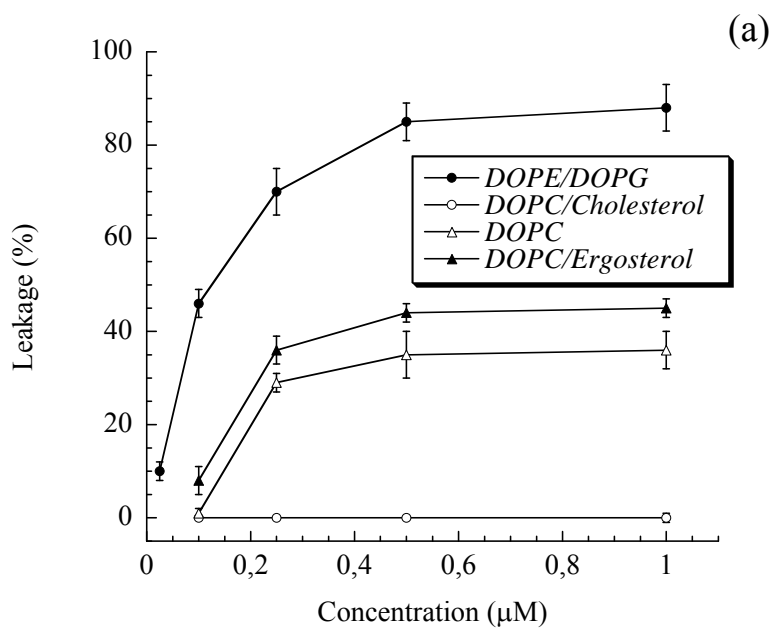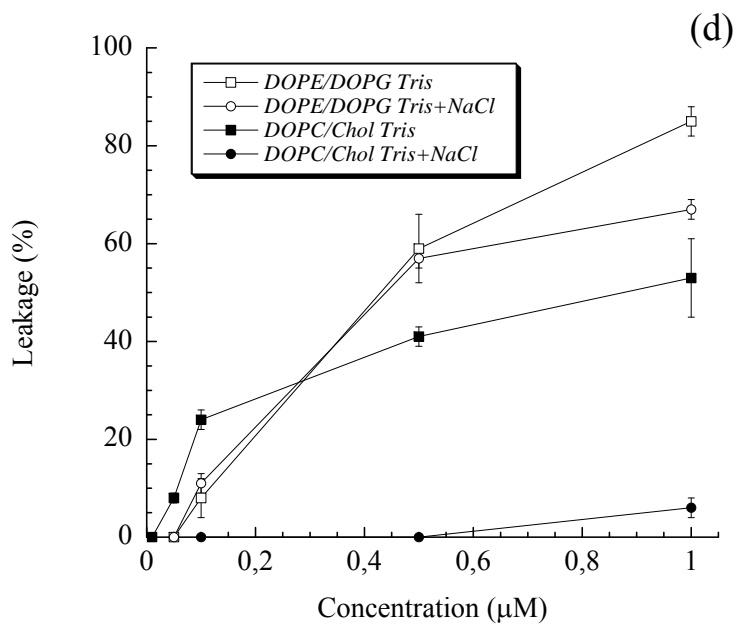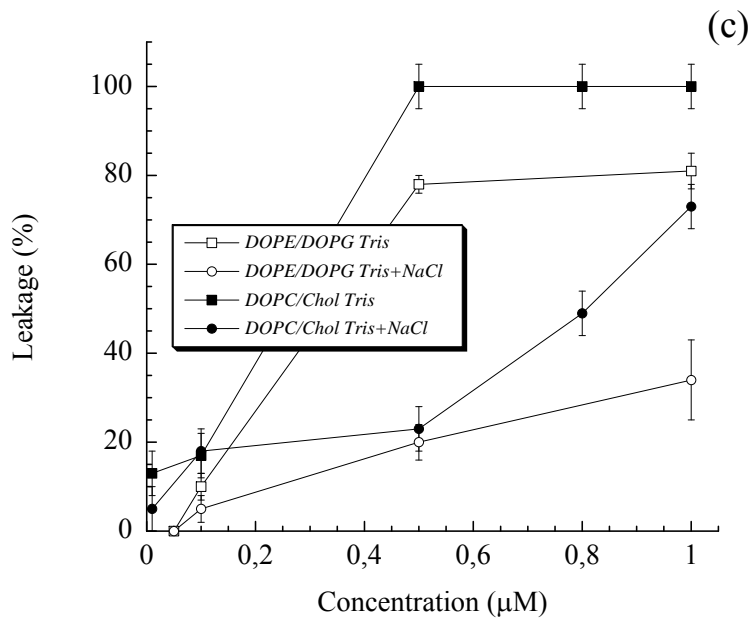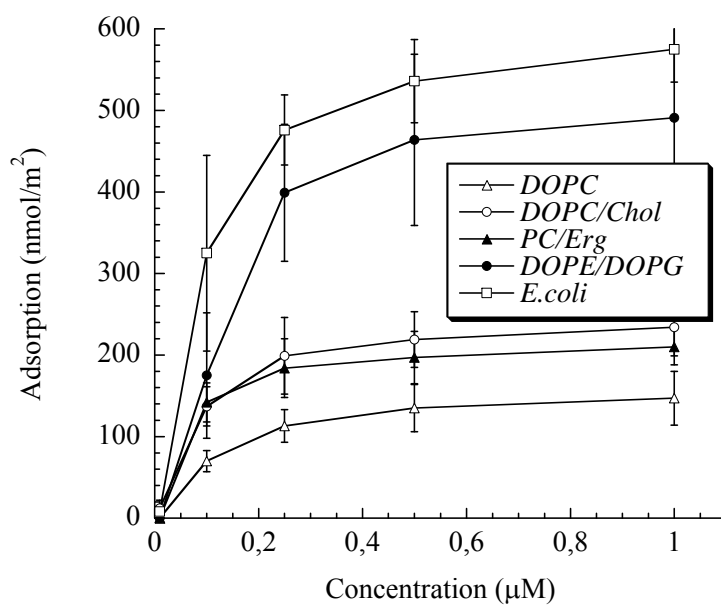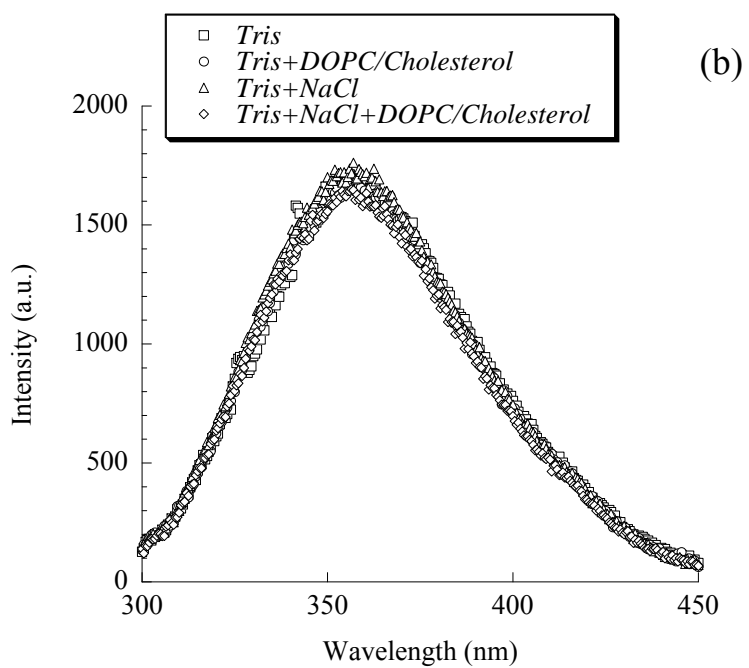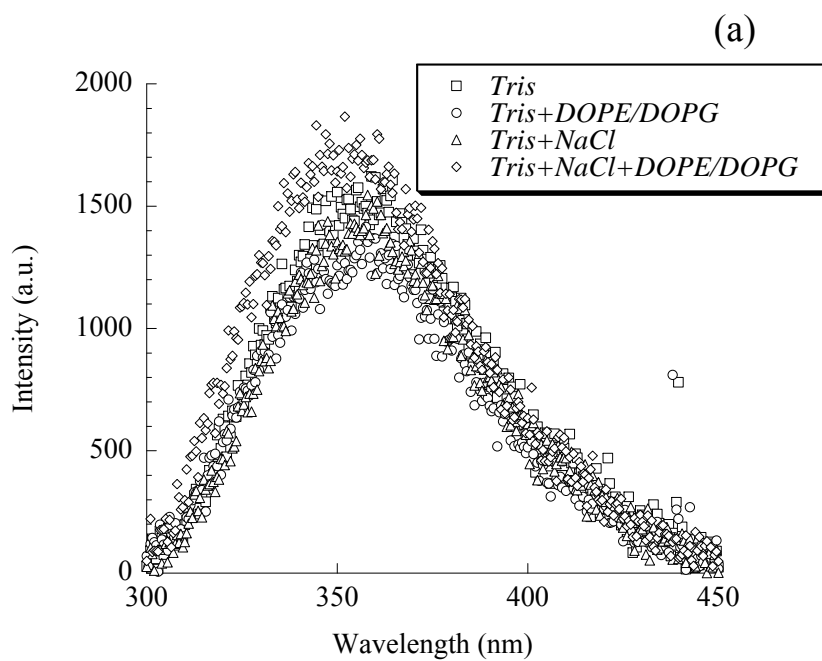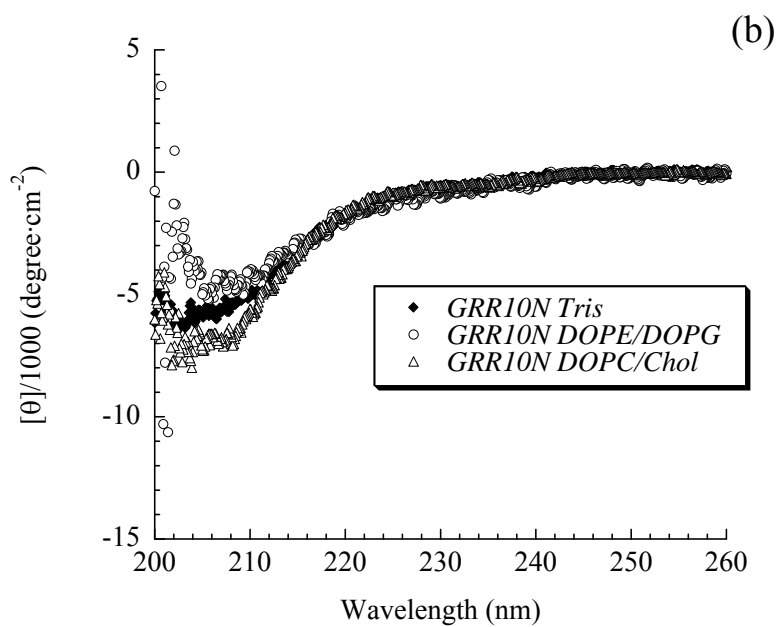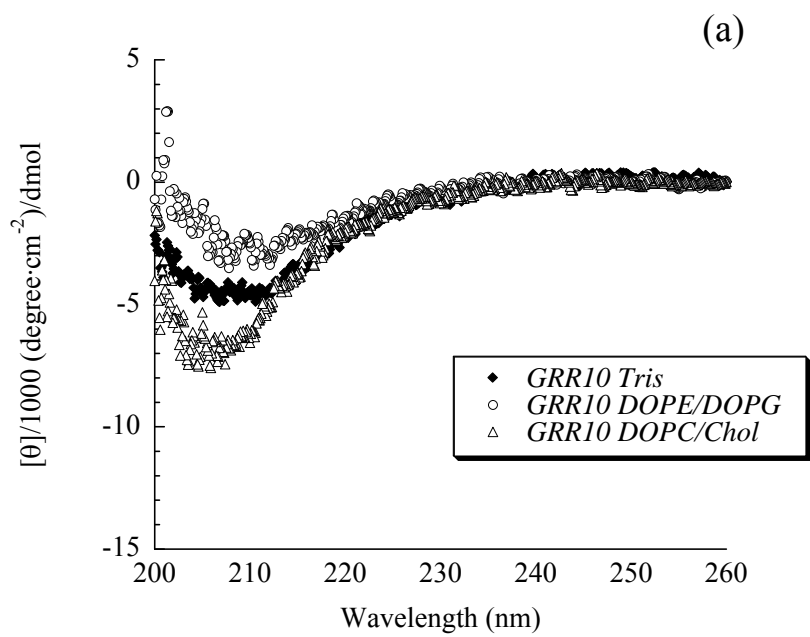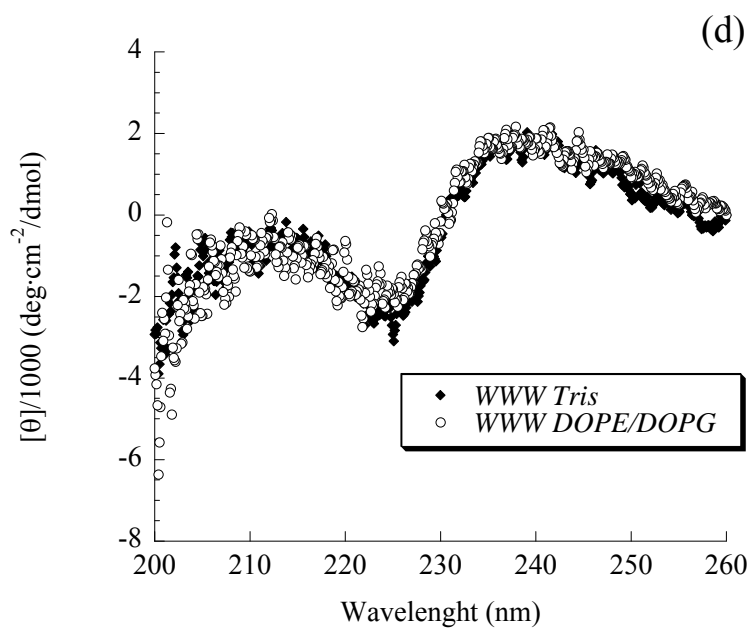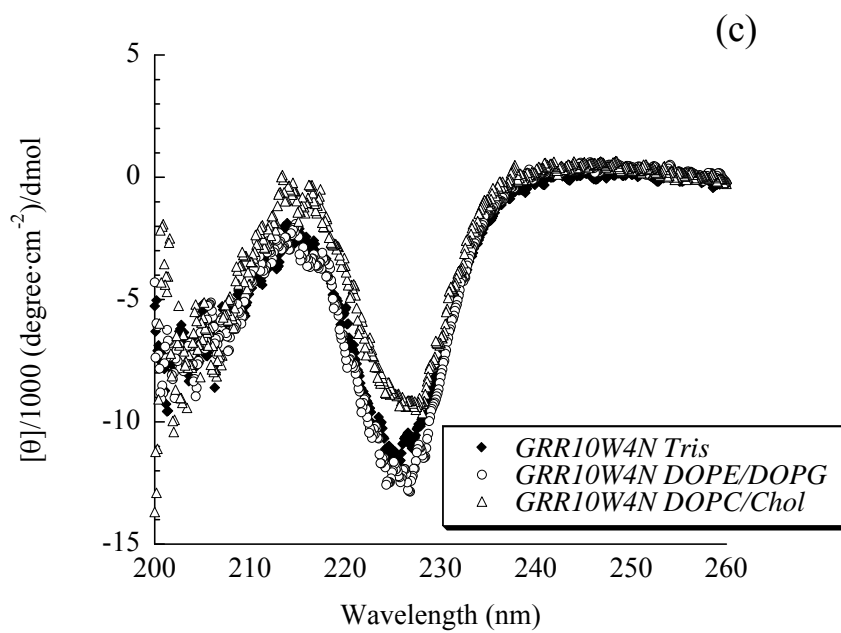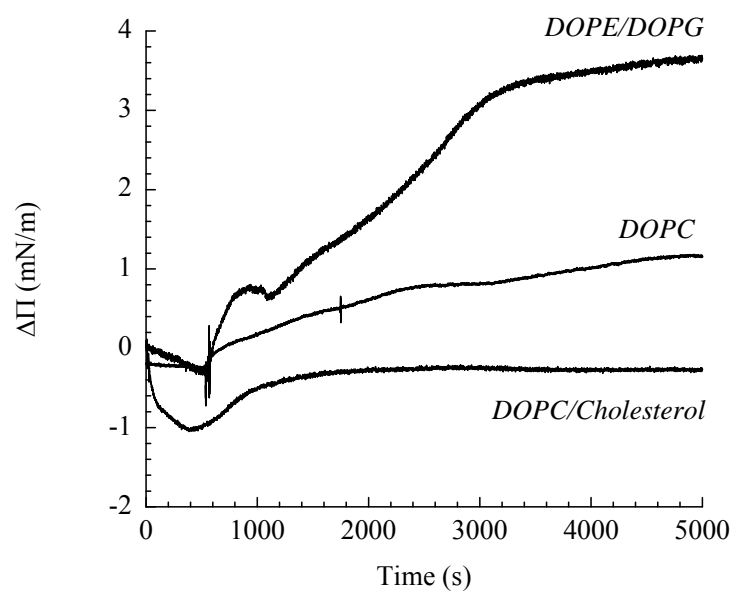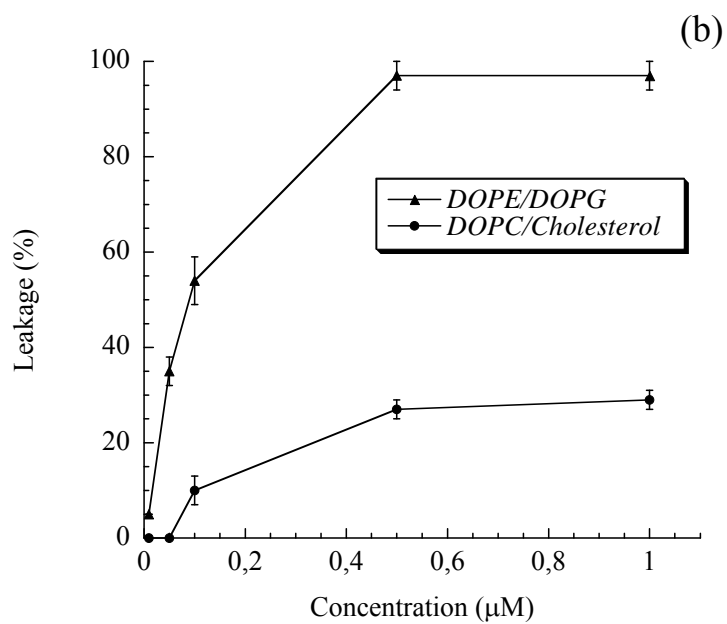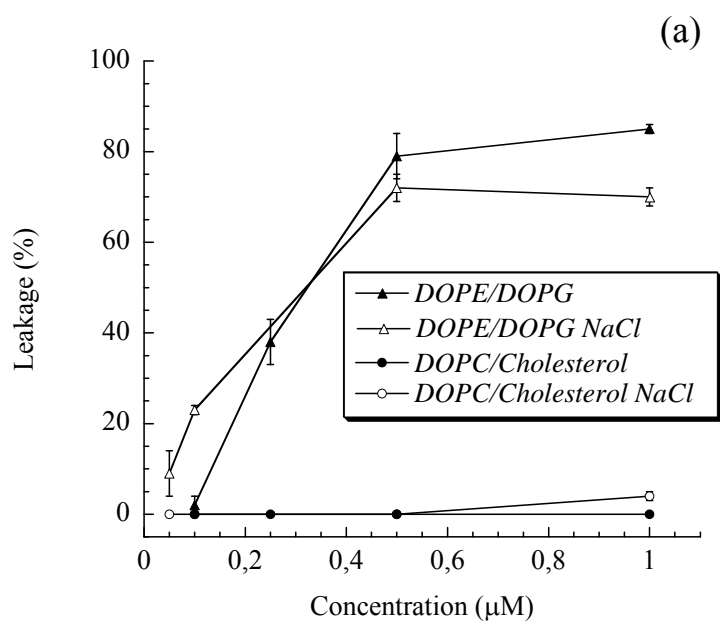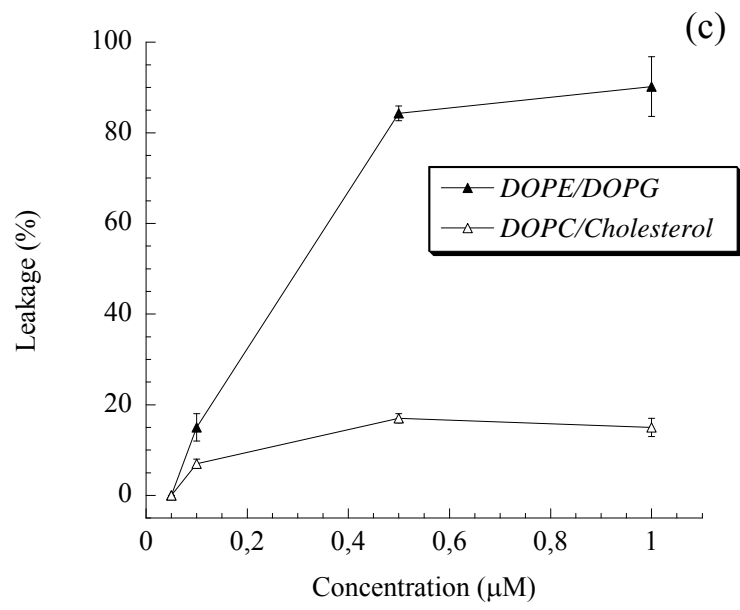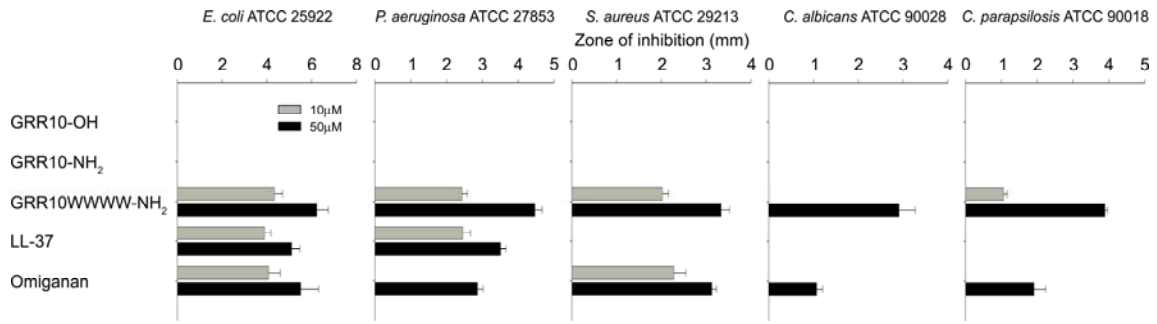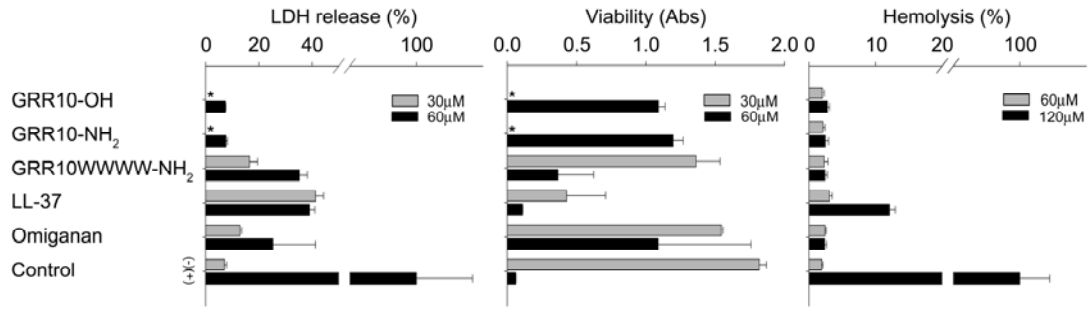
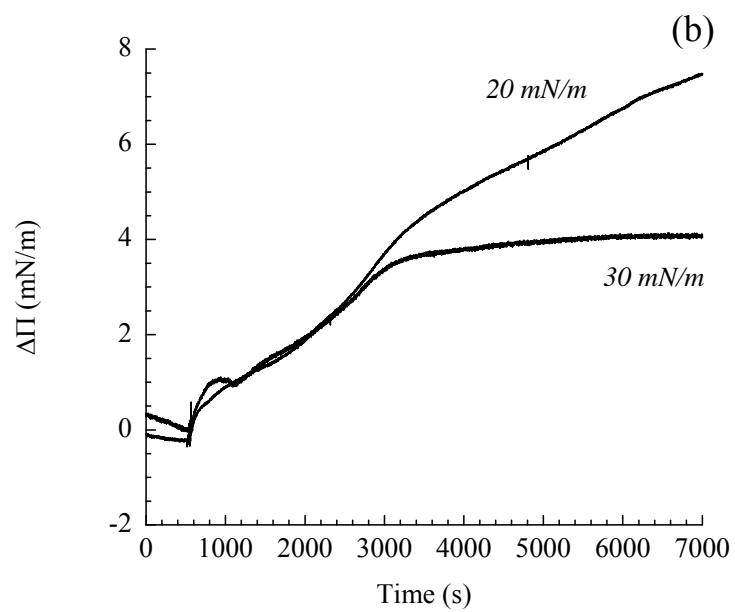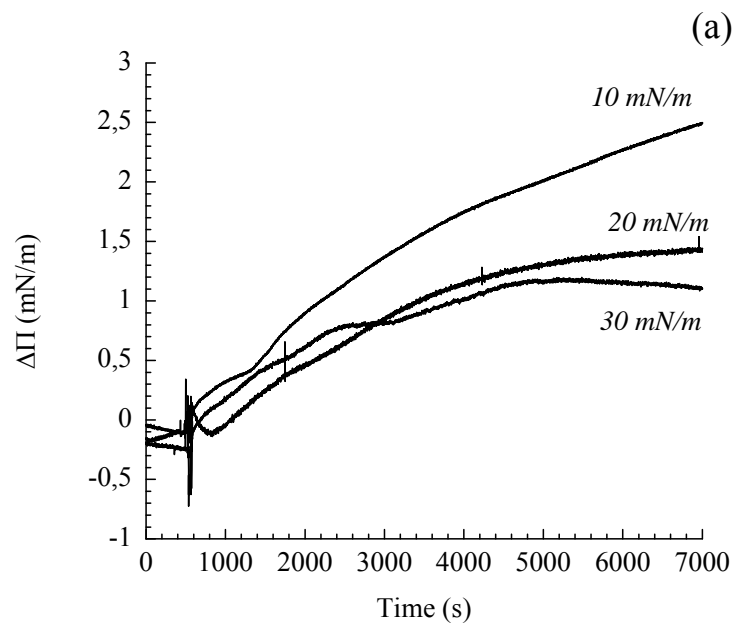Figure 7.

Figure 8.

Figure 9.

Supporting Material

Figure S1 Peptide-induced leakage of DOPE/DOPG liposomes for GRR10, GRR10N, and GRR10W4N at 10 mM Tris, pH 7.4, in the absence and presence of additional 150 mM NaCl. Leakage induction by the WWW tripeptide was 0±5% throughout the concentration span indicated.

Figure S2 Peptide-induced leakage of *E. coli* liposomes for GRR10N and GRR10W4N at 10 mM Tris, pH 7.4, in the absence (a) and presence (b) of additional 150 mM NaCl.
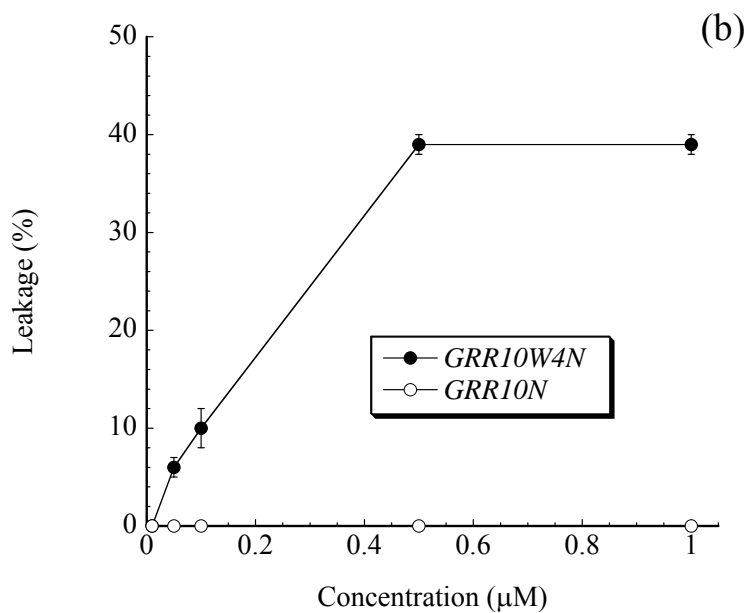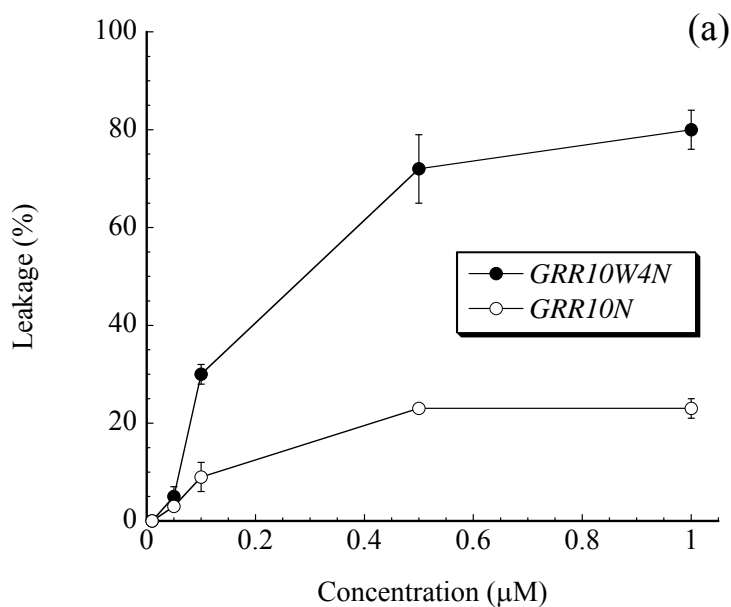
Figure S3 Effects of surface pressure on incorporation of GRR10W4N in DOPC (a) and DOPE/DOPG (b) monolayers at 10 mM Tris, pH 7.4.

Figure S3 Effects of surface pressure on incorporation of GRR10W4N in DOPC (a) and DOPE/DOPG (b) monolayers at 10 mM Tris, pH 7.4.

Figure S4 Antimicrobial effect, as determined by radial diffusion assay (RDA) in 10 mM Tris, pH 7.4, with additional 150 mM NaCl, GRR19F5 (10 and 50 µM) against *E. coli* ATCC 25922, *P. aeruginosa* ATCC 27853 and *S. aureus* ATCC 29213. For comparison, corresponding data for the control peptide GRR10 are included as well. In RDA, peptides are placed in wells in agar gels containing confluent microbes. On radial diffusion, the peptide will kill bacteria and result in a clearance zone containing disintegrated microbes. Thus, the higher the diameter (d), the higher the growth inhibition, i.e., the more potent the peptide.
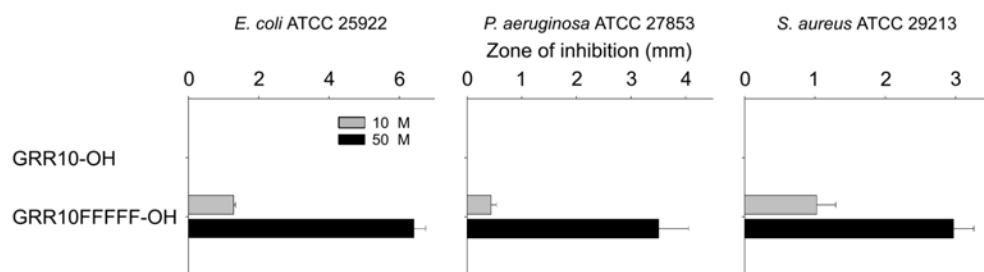
Figure S5 Viable count assay (VCA) of GRR10W4N for *P. aeruginosa* ATCC 27853 and *S. aureus* ATCC 29213 ($2*10^6$ cfu/ml) in buffer containing 20% citrate plasma, at the indicated peptide concentrations.
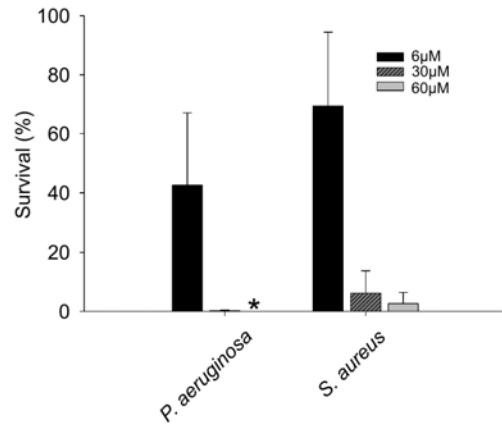
Table S1 Minimum inhibitory concentration (MIC; μM) values of the indicated peptides under NCSLA protocol.

	E. coli ATCC 25922	*S. aureus ATCC 29213*	*P. aeruginosa ATCC 27853*
GRR10	>160	>160	>160
GRR10N	>160	>160	>160
GRR10W4N	20	40	20
GRRF5	20	2.5	20
Omiganan	20	10	20
LL-37	10	10	10